



THE INFLUENCE OF SCALE AND MATERIAL ON THE DAMPING FACTOR BY SIMILITUDE CONDITIONS

Maria Lúcia M. Duarte

Universidade Federal de Minas Gerais (UFMG); Depart. Engenharia Mecânica (DEMEC)
Av. Antônio Carlos, 6627 – Pampulha – Belo Horizonte/MG, Brasil, CEP:31270-901
e-mail: mlduarte@dedalus.lcc.ufmg.br

Abstract. *This paper investigates the influence of scale and material on the damping factor of structures. In order to evaluate that, two different types of structures were fabricated in laboratory. For these prototypes, reduced scale models were designed and constructed according to the structural elastic similitude conditions, using different scales and materials. Also, the number of joints were varied for the two prototypes. It can be observed from the results presented in this paper that the damping factor depends strongly on the material used whereas there is no influence due to the scale adopted. However, it should be noticed that all tested structures have linear behaviour and no attempt was made to control the joints stress level.*

Key-Words: *Similitude conditions, Damping factor, Experimental Analysis, Structures*

1. INTRODUCTION

Damping in structural systems has been the subject of research for many years – as far back as 1959, when there was an Annual Meeting of the ASME, in Atlantic City (Ruzicka (1959)). Although the literature seems to be old, many interesting papers may be found there.

Lazan (1959), for example, defined the various types of damping in his work. There, the component parts of a system and the damping configuration were analysed considering certain types of structural damping mechanisms of particular interest. Representative values of damping for several materials and some points related to their engineering interpretation were presented. Mentel (1959) showed a study about the vibration energy dissipation on structural support joints. He concluded that the dissipation of energy on the panel supports could, in certain cases, exceed the damping inherent to the material by several orders of magnitude. Marin and Sharma (1959) presented several experimental techniques for the calculation of damping. He mentioned that the logarithmic decrement is the simplest technique to be used and, as long as care is taken, it can provide very reliable results.

Structural damping is still not fully understood today and so, more detailed research on this subject is of primary interest. The objective of the work presented here is to use models and prototypes tested in laboratory, to verify the influence on the damping factor of the reduced modelling of structures based on the similitude theory. For that, two different types of structures were used: the simplified structure (with the smallest number of joints possible and well defined boundary conditions) and the framed structure (with a higher number of joints and also well defined boundary conditions). Care was taken to design a support that was the

closest possible to a perfect clamping, in order to reduce the Coulomb damping inherent to supports. No control was performed on imposed displacements or tension levels.

This paper is organised as follows: section 2 presents the basis for the similitude theory. This is followed by the definition of the prototype and models in section 3. After that, the results for the frequency updating necessary for the model corrections are shown (section 4), followed by the obtained damping factors for each structure studied (section 5). Finally, some conclusions are drawn in section 6.

2. SIMILITUDE THEORY

The design of the reduced models was made in accordance with the structural elastic similitude theory (Roitman et al, 1989; Duarte, 1990). A brief overview of the process is presented below. First, it is necessary to find the non-dimensional parameters. Then, the scale factors can be derived from these.

2.1 Non-dimensional parameters

The physical parameters and the fundamental units involved in a dynamic problem of a structure vibrating on air are presented in Table 1. There, the physical parameters are: L (characteristic dimension: for example, length of the structure, geometric dimensions, etc.), E (Elastic modulus), ρ (specific mass), g (gravitational acceleration), T (period of oscillation), F (force: for example, weight of the structure, excitation force, etc.) and the fundamental units are: L (length), M (mass) and T (time), respectively. The rank of the dimensional matrix is $r = 3$ and the number of physical parameters is $n = 6$. Therefore, the number of non-dimensional parameters to be determined are $n-r = 3$.

Table 1. Parameters for the calculation of the non-dimensional variables

	L	E	ρ	g	T	F		
L	1	-1	-3	1	0	1	or	
M	0	1	1	0	0	1		$\alpha_1 - \alpha_2 - 3\alpha_3 + \alpha_4 + \alpha_6 = 0$
T	0	-2	0	-2	1	-2		$\alpha_2 + \alpha_3 + \alpha_6 = 0$
	α_1	α_2	α_3	α_4	α_5	α_6		$-2\alpha_2 - 2\alpha_4 + \alpha_5 - 2\alpha_6 = 0$

By making the values of α_4 , α_5 , α_6 in equation (1), each time one of them equals to unity and the others zero, it is possible to find the remaining α_i coefficients. These are the powers of the physical parameters for the determination of the non-dimensional parameters. For example, making $\alpha_4 = 1$, $\alpha_5 = \alpha_6 = 0$ will result from equation (1) in $\alpha_1 = 1$, $\alpha_2 = -1$ and $\alpha_3 = 1$. Following the same argument, one arrives to the non-dimensional parameters, as given below:

$$\pi_1 = \frac{L\rho g}{E}; \quad \pi_2 = \frac{T}{L} \sqrt{\frac{E}{\rho}} \quad \text{and} \quad \pi_3 = \frac{F}{EL^2} \quad (2)$$

The other non-dimensional parameter is related to the damping factor (ζ) of the structure:

$$\pi_4 = \zeta \quad (3)$$

When the models are designed respecting the scale factors for the stiffness and mass of the structure, it has been assumed that equation (3) is satisfied approximately (Roitman et al, 1989). This may not be true, since the damping factor may be related to the material used to construct the model. The verification of this hypothesis is the main objective of this paper.

2.2 Scale factors

In order to design the models according to the similitude theory, it is necessary that the non-dimensional parameters of equations (2) to (3) take the same value for both the models and the prototypes. So, from π_1 (equation (2)):

$$\frac{K_L K_\rho K_g}{K_E} = 1 \quad (4)$$

Assuming $K_g = 1$, equation (4) yields the specific mass scale:

$$K_\rho = \frac{K_E}{K_L} \quad (5)$$

From π_2 (equation (2)) and equation (5), the period (or frequency) scale is obtained:

$$K_T = \sqrt{K_L} \quad \text{or} \quad K_f = \frac{1}{\sqrt{K_L}} \quad (6)$$

From π_3 (equation (2)) and equation (5), one finds the force scale (i.e., weights), consequently, masses (where m is the mass of one element of the structure):

$$K_F = K_\rho K_L^3 \quad \text{or} \quad K_m = K_\rho K_L^3 \quad (7)$$

For the flexural stiffness of the structure (EI), assuming that $K_I = K_L^4$ (where I is the moment of inertia of the cross section), one gets after using equation (5):

$$K_{EI} = K_\rho K_L^5 \quad (8)$$

Equation (8) is very difficult to satisfy in practice without correcting the specific mass of the model – even when using the distorted scale for the thickness of the adopted tube walls (K_d), i.e., $K_d \neq K_L$. This is because the thickness of commercial tubes are normally greater than that calculated through the similitude theory, resulting in a greater moment of inertia than that calculated using equation (8). It is possible to compensate for the increase of stiffness, by increasing the mass of the element. This can be obtained by using equations (7) and (8):

$$K_{EI/m} = K_L^2 \quad (9)$$

So, using equations (7) to (9) and the area (A) scale factor ($K_A = K_L^2$), the specific mass scale factor used in the design of the models is finally obtained:

$$K_\rho = \frac{K_E K_I}{K_A K_L^3} \quad (10)$$

3. PROTOTYPE AND MODELS: DEFINITIONS

3.1 Simplified structure

The simplified structure was thought as an structure with the smallest possible number of

joints. Due to the difficulty of fixing just a single bar, a modification to the original design was necessary so that it became an inverted “T” structure, as shown in Figure 1. Figures 2 and 3 show a detail of the support of this structure for both the prototype and models, respectively. Its main geometrical and mechanical dimensions are presented in Table 2, where: L (tube length), ϕ_{ext} (external diameter), d (tube thickness) and $\rho_{S,T}$ (specific mass calculated using the similitude theory). The other specific masses will be explained later in the text.

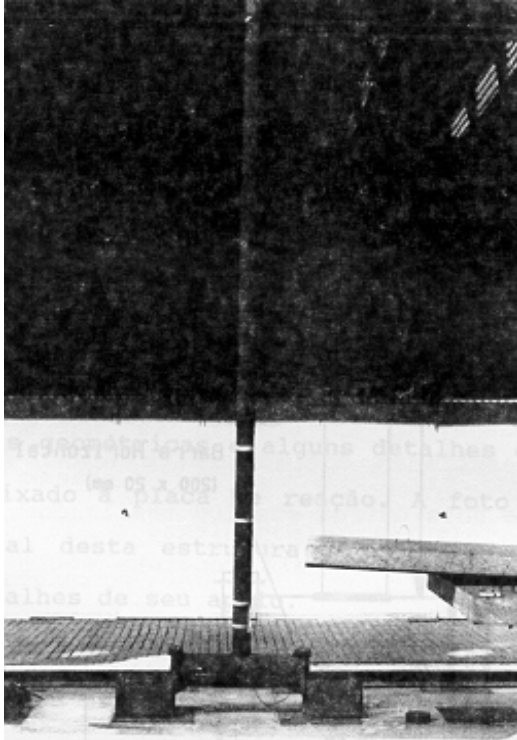
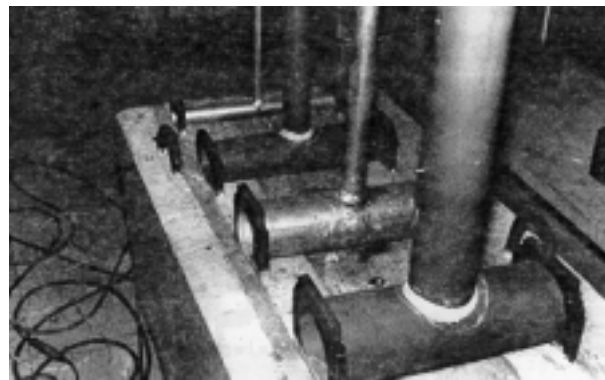
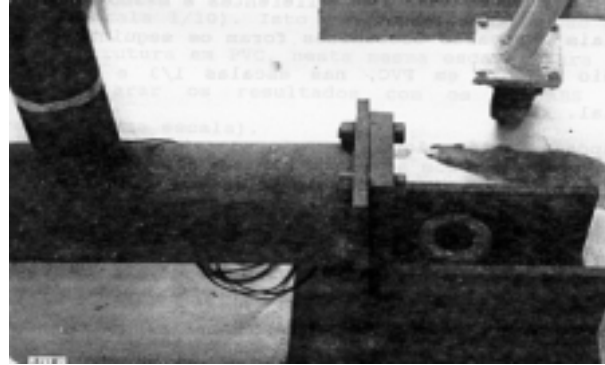


Figure 1 – General view of the simplified prototype structure



Figures 2 and 3 – Details of the support for the simplified prototype and model structures

Eight models were designed using different materials (two metals and two plastics) and geometric scales (1/3, 1/5 and 1/10). The main characteristics of these are also presented in Table 2 and followed the similitude theory, as presented in the previous section.

For the first four models [aluminium (1/3 and 1/5) and PVC (1/3 and 1/5)], the modelling was made only for the vertical bar, since the horizontal bar was assumed to have flexural stiffness infinitely greater than the vertical one. For the horizontal bar, it was only assumed a diameter approximately double that for the prototype (all with the same length). For the vertical bars, besides respecting the geometric scale, equation (9) was also satisfied through the correction of the specific mass of each element (equation (10)). The external diameter for the aluminium models bars were only modelled approximately according to the geometric scale. For the PVC models it was not possible to reduce the external diameter since there was no tube with such characteristics.

For the following four models [stainless steel (1/3 and 1/5), PVC (1/10) and ABS (1/10)] the modelling was made for both vertical and horizontal bars. The specific mass was not corrected for the latter though, since it did not influence the values of the damping factor. The external diameter scale factor was not followed only for the PVC model for the same reason already mentioned.

The specific mass calculated through the similitude theory was completely followed in the majority of the models by correcting the difference between the theoretical ρ and the

weighed ρ . This was achieved by altering the necessary additional mass (distributed along the vertical bar). For the ABS model, the weighed value was greater than that from the similitude theory. That would result in a decrease on the model weight, achieved either by decreasing the cross section of the vertical bars or by making holes along its length. As the difference was not considered high and the two methods would decrease the flexural stiffness of the bars, nothing was done in that respect. The welding (gluing for the ABS model) of the horizontal and vertical bars was carefully performed to prevent micro cracks which could influence the damping results obtained.

Table 2. Physical and mechanical characteristics of prototype (PT) and models used

	Ma- terial	Simplified Structure							Framed Structure					
		Mech. Prop.	Bar	L	ϕ_{ext}	d	$\rho_{S.T}$	ρ_{final}	Bar	ϕ_{ext}	d	$\rho_{S.T}$	$\rho_{reached}$	ρ_{final}
PT	Steel	$E = 210$	Vert.	486,5	101,6	6,35			Legs	33,4	4,55	10,34		
		$\rho = 7,86$	Horiz.	78	200	20			Horiz.	21,34	2,77	7,86		
1/3	A	$E = 69$	Vert.	1621,7	31,75	3,175	6,33	4,97	Legs	12,7	1,58	10,31	14,55	16,45
		$\rho = 2,71$	Horiz.	274	88,9	2,38	x	x	Horiz.	9,53	1,59	17,06	2,71	x
	SS	$E = 210$	Vert.	1621,7	32	1,25	22,06	13,30	Legs	12,7	1,0	34,3	40,4	23,27
		$\rho = 7,97$	Horiz.	273	63,5	1,5	x	x	Horiz.	7,94	0,7	41,9	7,97	x
PVC	$E = 3$	Vert.	1621,7	75	5,75	1,61	1,18	Legs	32	3,3	2,97	3,2	4,26	
	$\rho = 1,46$	Horiz.	274	110	5,0	x	x	Horiz.	20	1,5	3,9	1,46	x	
1/5	A	$E = 69$	Vert.	973	15,87	2,0	6,96	4,53						
		$\rho = 2,71$	Horiz.	274	31,75	3,175	x	x						
	SS	$E = 210$	Vert.	973	19,05	1,0	35,23	34,23						
PVC	$E = 3$	Vert.	973	40	4,125	2,01	1,23							
	$\rho = 1,46$	Horiz.	274	75	5,75	x	x							
1/10	ABS*	$E = 3$	Vert.	486,5	11,1	1,6	1,14	1,18	Legs	25,4	1,6	2,02	2,01	1,13
		$\rho = 1,05$	Horiz.	63	25,4	1,6	x	x	Horiz.	11,1	1,6	1,05	1,05	x
1/10	PVC	$E = 3$	Vert.	486,5	20	3,65	3,46	3,56						
		$\rho = 1,46$	Horiz.	63	25	2,975	x	x						

Notes: A = aluminium; SS = Stainless Steel. Units: E [GPa], ρ [g/cm^3], L [mm], ϕ [mm], d [mm]

* For the ABS framed structure, the geometric scale was 1/3.

3.2 Framed structure

In order to verify the influence of joints on the damping factor, a spatial framed prototype structure was devised, clamped on the base and free on the top. It has a rectangular cross section to prevent coupling of natural frequencies in the two main directions. It was made of continuous tubes for the legs and horizontal bars, equally spaced, as shown in Figure 4. The results were obtained for the direction of smaller stiffness (y axes, Figure 4).

For the reduced models, only the 1/3 geometric scale was assumed this time, as the scale showed to have no importance on the damping factor, as will be seen in the following sections. However, when calculating the ABS model according to the similitude theory, there was no material available to respect this 1/3 scale. That fact forced the addition of mass on the horizontal bars of the prototype (as the $\rho_{S.T}$ for the ABS structure was smaller than the theoretical value). Then, the new specific masses of the prototype were assumed to be $10,34 \text{ g}/\text{cm}^3$ for the horizontal bars and $7,86 \text{ g}/\text{cm}^3$ for the legs. These values were used to recalculate the models, as shown in Table 2 ($\rho_{reached}$). Nevertheless, when weighing the prototype, it was much heavier than previously calculated using the theoretical values (probably due to imper-

fections on the diameter) and so, it was not necessary to add any additional mass.

Figure 5 shows the framed model structures with details of their supports. The supports were designed in order to guarantee the design clamped condition. As for the previous structure, special care was taken with the welding (gluing) of the horizontal bars to the legs to prevent micro cracks that could spoil the results.

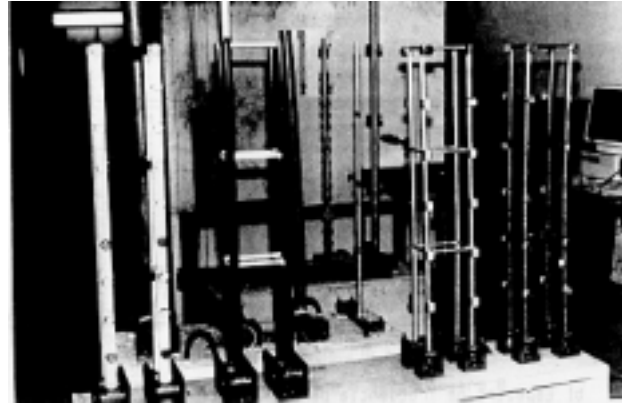
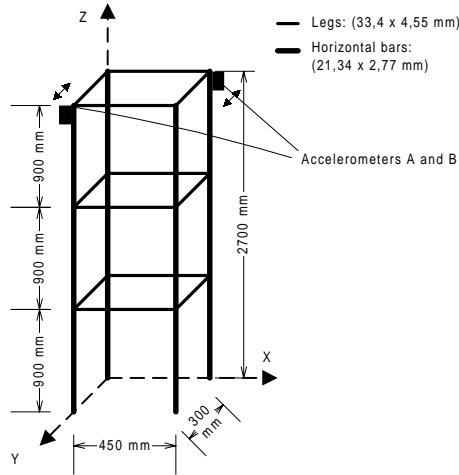


Figure 4 – Sketch of the framed prototype structure

Figure 5 – Framed models after frequency updating (with a view of the supports)

The geometric scale for the models was respected, as well as the scale given by equation (9). The latter was achieved by correcting the specific mass of the models (equation (10)). The scales for areas and external diameters were followed whenever possible. Again, it was necessary to use distorted scale for the thickness of the tube walls in most models, for the same reasons mentioned for the simplified structure. The characteristics of the models are also presented in Table 2, where the $\rho_{reached}$ column is the reached specific mass obtained after the addition of mass on the horizontal bars.

4. FREQUENCY CORRECTION

It was necessary, after constructing the models, to correct their experimental natural frequencies so that they would match the values obtained for the prototype when using the similitude theory (K_f , equation (6)). These natural frequencies were obtained from free vibration tests. Only one accelerometer was used for the simplified structures, whereas the framed ones used two accelerometers (in opposite directions, as shown in Figure 4). The latter was necessary so that it would be possible to distinguish between flexural and torsional modes.

4.1 Simplified structure

Initially, the theoretical and experimental natural frequencies were compared. The theoretical values were calculated using clamped-free cantilever beam formulas (Clough and Penzien, 1975). The results are shown in Table 3 and validate the hypothesis of a clamped-free system. The differences found for the prototype can be explained by the differences between the real and theoretical mechanical and geometrical characteristics used. As the main objective of the study was to correlate the experimental natural frequencies of the prototype and models, no effort was made to better correlate the theoretical and experimental values given for the prototype.

The correction for the natural frequencies of the models was made by taking into account

the frequency scale, as given by equation (6). The objective was to get an experimental natural frequency which was the closest possible to that calculated using this equation. This was achieved through the modification of the additional mass for each model, which changed the final specific mass of the models (ρ_{final}), as seen in Table 2. Comparison of ρ_{final} and $\rho_{S.T.}$ columns shows that the former is smaller for the great majority of the models. This fact can be explained by the variations between the theoretical and real values of the geometric and mechanical characteristics, as happened for the prototype. Another explanation can be the difficulty in modelling at the same time the flexural and axial stiffness (here, only the former was considered). Comparing the values of the natural frequencies of the models calculated from the experimental frequency of the prototype ($f_{S.T.}$ and $f_{exp.}$) as shown in Table 3, it can be concluded that the models are in accordance with the physical similitude condition. The only structure in which this was not true was for the ABS model (as it required mass to be taken from the structure and this was not done). The theoretical values presented in Table 3 were calculated considering the final specific mass of each model, as given in Table 2. An attempt was made to correct the elastic modulus used for the models, which gave a better theoretical/experimental correlation. For the ABS model, only the first natural frequency had a good correlation, as the other frequencies were influenced by the mass of the accelerometer (also a problem for the PVC model – 1/5 scale). Comparing the theoretical and experimental values given in Table 3, it can be concluded that they correlated satisfactorily.

Table 3. First three natural frequencies (Hz) of the simplified structure (theoretical –T, similitude theory – S.T. and experimental – exp.) – Prototype and Models

Scale	Material	f_1			f_2			f_3		
		f_T	$f_{S.T.}$	$f_{exp.}$	f_T	$f_{S.T.}$	$f_{exp.}$	f_T	$f_{S.T.}$	$f_{exp.}$
Ptype	Stell	4,08	x	4,8±0,8	25,6	x	27,2±0,8	71,69	x	66,4±0,8
1/3	Aluminium	7,3	8,3±0,1	7,2±0,4	45,7	47,1±0,1	45,2±0,4	127,9	115,0±0,1	129±1
	Stainless Steel	8,1	8,3±0,1	7±1	51,1	47,1±0,1	46±1	143,0	115,0±0,1	136±1
	PVC	7,4	8,3±0,1	7,2±0,4	46,3	47,1±0,1	44,8±0,4	129,6	115,0±0,1	129±1
1/5	Aluminium	10,1	10,7±0,2	9,6±0,4	63,4	60,8±0,2	55,6±0,4	177,7	148,5±0,2	158±1
	Stainless Steel	9,3	10,7±0,2	8±1	58,1	60,8±0,2	55±1	162,6	148,5±0,2	157±1
	PVC	10,4	10,7±0,2	8,8±0,8	65,4	60,8±0,2	56±0,8	183,2	148,5±0,2	148±1
1/10	ABS	11,4	15,2±0,3	11±1	71,3	86,0±0,3	54±1	199,6	210,0±0,3	166±1
	PVC	13,4	15,2±0,3	14±1	83,7	86,0±0,3	88±1	234,3	210,0±0,3	220±1

4.2 Framed structure

The same steps mentioned for the simplified structure were used here. The theoretical determination of the natural frequencies was performed this time through the use of two programs based on Finite Element Method: SAFE (Torres, 1988) and OMEGA (Torres, 1988). For the experimental values, when analysing the frequency spectrum of each accelerometer and the relative phase plot between them, it is possible to see if the modes are bending or torsional modes (if the relative phase for the frequencies are close to 0^0 or 180^0 , respectively).

Table 4 shows the values for the first three bending (B) and torsional (T) natural frequencies of the framed structure. There, analysing the results for the prototype structure, it can be seen that only the lower modes present good correlated (the higher modes were probably affected by the precision of the numerical calculation). As the main interest was the lower modes (for which the natural frequencies were corrected), no attempt was made to better correlate the higher ones.

It was also necessary to correct the natural frequencies of the framed structure models, so to follow the frequency scale factor (equation (6)). The same procedure used for the simpli-

fied structure was employed here. The final specific mass for the legs (since the additional mass was distributed only for those elements) is given in Table 2. For the horizontal bars, the theoretical values were used. The discrepancies found between the final (ρ_{final}) and reached ($\rho_{reached}$) specific masses can be explained in the same way as for the simplified structures. Comparing now the frequency values from the similitude theory and experimental tests it can be seen a good correlation between them. As a final comparison, the theoretical frequencies found using the final specific mass (f_T for the models) are compared with the experimental ones. There was also an attempt to adjust the elastic modulus (E) for a better theoretical/experimental correlation and the results presented in Table 4 already take that into account. However, the stainless steel and PVC models did not need this adjustment. Again, the lower modes were better predicted than the higher ones and the same comments made previously apply here.

Table 4. First three natural frequencies (Hz) of the framed structure (theoretical –T, similitude theory – S.T. and experimental – exp.) – Prototype and Models

f	Mode Type	Prototype			Models							
		f_T	$f_{exp.}$	$f_{S.T.}$	A		SS		ABS		PVC	
					f_T	$f_{exp.}$	f_T	$f_{exp.}$	f_T	$f_{exp.}$	f_T	$f_{exp.}$
1 st	B	9,12	9,12±0,08	15,8±0,1	16,92	15,2±0,8	17,66	15,2±0,8	16,44	13,6±0,8	14,34	15,2±0,8
	T	15,08	17,6±0,4	30,7±0,7	24,37	23,2±0,8	32,8	28,0±0,8	33,27	31,2±0,8	24,05	28,8±0,8
2 nd	B	30,12	32,0±0,4	55,4±0,7	52,28	52,0±0,8	58,22	54,4±0,8	60,5	59,2±0,8	50,11	59,2±0,8
	T	42,19	51,2±0,8	88,7±1,4	68,98	72,8±0,8	88,72	80,8±0,8	87,99	87,2±0,8	68,65	88,0±0,8
3 rd	B	53,32	67,2±0,8	116,4±1,4	83,75	108±2	102,1	122±2	119,2	142±2	94,56	128±2
	T	62,82	86,4±0,8	149,6±1,4	99,54	134±2	126,3	146±2	122,8	166±2	106,1	158±2

5. DAMPING FACTORS

In order to find the damping factors for the tested structures, two types of testes were performed: free and forced vibration tests. When using the former, only the damping factor associated to the first flexural mode of the structure can be calculated through the use of the logarithmic decrement technique (Clough and Penzien, 1975). When using the latter, all damping factors of the structure can be calculated through the use of modal analysis techniques (Ewins, 1984). Among the several available techniques, the circle-fit was chosen to be used here.

5.1 Logarithmic decrement results

The logarithmic decrement method was used to calculate the damping factors for the first flexural mode of the structures. However, although using a lower band pass filter (which cuts frequencies immediately above the first natural frequency), some time signals were still coupled. So, it was necessary to adjust the envelop of the signal prior to the use of the technique. A least square fit technique was used for that purpose. Figure 6 shows such an example for the framed stainless steel 1/3 model, with the least squares fit presented in Figure 7.

The damping factors were obtained from at least three time signals to average the imperfections inherent in the experimental data. The values are presented in Table 5, ζ (%). It can be observed from the results that the damping factors are very distinct for the metal and plastic structures. It has got not so much variation related to the scale factor. The damping factors obtained for the same material but for different structures showed a tendency to an increase in value with the increase of the number of joints. However, other studies not presented here (Duarte, 1990) with a much higher number of joints, showed that was not the real case. The quality of the fit (r) was monitored for all structures to guarantee the confidence in the results. They were found to be very close to the ideal value of 1,00, as can be seen in Table 5.

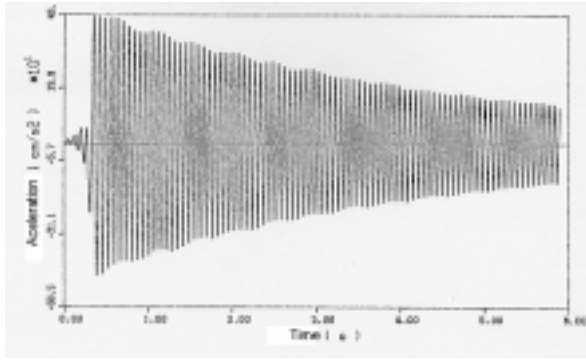


Figure 6 – Acceleration time signal for the framed stainless steel model (1/3 scale)

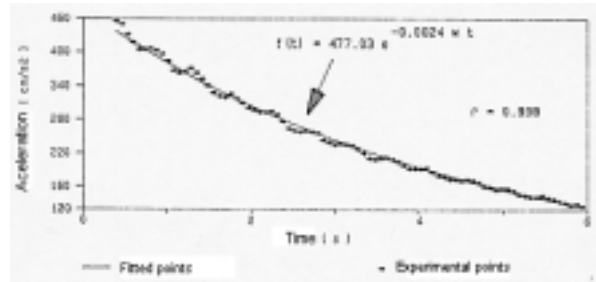


Figure 7 – Least square fit of the time signal shown in Figure 6.

Table 5. Damping values (ζ [%]) and correlation coefficients (r) from logarithmic decrement and damping values for the first three modes from circle-fit techniques

Structure \Rightarrow	Material \Downarrow	Logarithmic decrement				Circle-fit		
		Simplified		Framed		Simplified		
		ζ_1	r	ζ_1	r	ζ_1	ζ_2	ζ_3
Ptype	Steel	0,12	0,995	0,12	0,988	x	0.07±0.03	0.10±0.02
1/3	Aluminium	0,06	0,986	0,18	0,971	x	0.07±0.01	0.10±0.01
	Stainless S.	0,06	0,997	0,24	0,998	x	0.11±0.01	0.18±0.03
	PVC	0,88	0,999	1,83	0,997	0.88±0.01	1.28±0.02	1.60±0.01
1/5	Aluminium	0,15	0,989			x	0.22±0.03	0.18±0.04
	Stainless S.	0,11	0,990			0.15±0.04	0.06±0.01	0.14±0.04
	PVC	1,16	0,998			1.44±0.22	1.62±0.02	2.08±0.01
1/10	ABS*	1,32	0,999	1,32	0,999	1.14±0.14	0.82±0.02	1.91±0.09
	PVC	1,11	0,998			1.16±0.14	1.99±0.04	2.33±0.11

* For the ABS framed structure, the geometric scale was 1/3.

x It was not possible to perform the test due to the coupling between the transverse frequencies.

5.2 Modal Analysis results

The results obtained from the circle-fit technique for the simplified structure are also presented in Table 5. Comparing the first mode values from this technique with the ones obtained from the logarithmic decrement, it can be seen that the correlation was quite good. So, for the structures where it was not possible to obtain the values through forced vibration, one can consider the value obtained from the free vibration .

Analysing the results as the mode number increases, it can be seen that, for the majority of the structures, the damping factor also increases. Only for the ABS 1/10 model and the stainless steel 1/5 model the above observation was not true. In order to conclude something in that respect it would be necessary to have more modes and this was not the case here. Again, the damping factors for metals and plastics were quite different. The results obtained from the circle analysis for the framed structure followed the same conclusions already made for the simplified structure (although they are not shown here).

Table 6 presents a summary of the results obtained for each of the structures studied. Analysing the results, it can be seen that the damping factor does not vary significantly with the mode analysed. Moreover, for the same materials the damping values are quite close, whereas for different materials they vary significantly. Also, it can be seen that the scale has

not much influence in such parameter.

Table 6. Summary of damping values found for the studied structures

Flexural Mode	Simplified Structures					Framed Structures				
	Metals		Plastics			Metals		Plastics		
	Ptype	Models				Ptype	Models			
Steel	Aluminium	Stainless S.	ABS	PVC	Steel	Aluminium	Stainless S.	ABS	PVC	
1 st	0.12	0.06→0.15	0.06→0.15	1.14	0.88→1.44	0.16	0.18	0.24	1.5	1.13
2 nd	0.07	0.07→0.22	0.06→0.11	0.82	1.28→1.99	0.10	0.17	0.19	0.95	1.63
3 rd	0.10	0.10→0.18	0.14→0.18	1.91	1.6→2.33	0.45	0.22	0.16	0.71	1.68
Variation	0.06→0.22			0.82→2.33		0.07→0.45			0.71→1.68	

6. CONCLUSIONS

It can be concluded from the results presented here that, for structures or models with linear behaviour, the damping factor depends strongly on the material of which they are made. The geometric scale has no influence on such parameter and so, it does not depend on the relation stiffness/mass. Moreover, only the variation of the distributed mass on the structure does not alter the damping factor. It was also verified that an increase on the number of joints of the structure does not affect significantly the values of the damping factors (they still depend strongly on the material used). However, further study is necessary in order to control the imposed displacements and stress levels applied to the structure so as to make the conclusions here more general.

REFERÊNCIAS

- Clough, R.W. and Penzien, J., 1975, "Dynamics of Structures", McGraw-Hill Kogakusha Ltda., Tokyo
- Duarte, M.L.M., 1990, "Estudo da Influência da Taxa de Amortecimento na Modelagem Reduzida via Teoria da Semelhança", Tese de M.Sc., Programa Engenharia Civil COPPE/ UFRJ, Rio de Janeiro, Brasil
- Ewins, D.J., 1984, "Modal Testing: Theory and Practice", Research Studies Press Ltd.
- Lazan, B.J., 1959, "Energy Dissipation Mechanisms in Structures, with Particular Reference to Material Damping", Proceedings of the ASME Annual Meeting, Atlantic City, New Jersey
- Marin, J. and Sharma, M.G., 1959, "Material Design for Resonant Members", Proceedings of the ASME Annual Meeting, Atlantic City, New Jersey
- Mentel, T.J., 1959, "Vibration Energy Dissipation at Structural Support Junction", Proceedings of the ASME Annual Meeting, Atlantic City, New Jersey, 1959
- Roitman, N., Batista, R.C. and Carneiro, F.L.L.B., 1989, "Reduced Scale Model for Fixed Offshore Structures", Experimental Mechanics, vol. 29, n. 3, pp. 372-377
- Ruzicka, J.E., 1959, "Structural Damping", Proceedings of the ASME Annual Meeting, Atlantic City, New Jersey.
- Torres, F.T., 1988, "Structural Analysis by Finite Element (SAFE)", Universidade Católica de Quito, Quito, Equador
- Torres, F.T., 1988, "Oscillation Modes and Single Value Analysis (OMEGA)", Universidade Católica de Quito, Quito, Equador